Journal of the Indian Society of Remote Sensing
https://doi.org/10.1007/s12524-022-01497-9

RESEARCH ARTICLE

Passive and Active Remote Sensing Data as Indicators of Vegetation Condition in Dry Woodland

Valeria E. Campos[1,2] · Viviana N. Fernandez Maldonado[1,2] · Emilce Amatta[2]

Received: 19 August 2020 / Accepted: 2 January 2022
© Indian Society of Remote Sensing 2022

Abstract
An important challenge is getting to know the condition of vegetation in dry woodlands, fragile ecosystems with high ecological value, to propose conservation strategies. Our objectives were: (1) to quantify on-the-ground vegetation composition and structure in dry *Ramorinoa girolae*-dominated woodlands on three study sites, using (A) field-based methods and (B) passive and active remotely sensed data at multi-scale and (2) to assess whether the integration of different remote sensors allows for a better estimation. We recorded field-based data on 36 plots of 50 × 30 m distributed in three sites (Ischigualasto $n = 16$; Valle Fértil $n = 10$; Private land $n = 10$). On each plot, we estimated the standard deviation (SD) of passive (EVI—Enhanced Vegetation Index—and SATVI—Soil Adjusted Total Vegetation Index) and active imagery data (SD of VV and VH polarisation) at multi-scale. The results of this approach show that passive and active remote sensing data were good indicators of almost all field-based data recorded at stand scale, except for richness, which was not related to remote sensing data. Shrub biomass, tree biomass and abundance of *R. girolae* were better explained by multi than single-sensor models. Only the variance in canopy cover of *R. girolae* was explained by single-sensor models. This work expands our understanding of the relationship of field-based data with both passive and active remotely sensed data, providing evidence that they could be used as a proxy for vegetation structure in dry *R. girolae*-dominated woodlands.

Keywords Optical remote sensing data · Synthetic-aperture radar imagery data · Vegetation composition · Vegetation structure · Dry *Ramorinoa girolae*-dominated woodlands

Introduction

Woodland conservation has been for many years, and continues to be today, the top agenda for many world conservation organisations, authorities and interest groups (Lawley et al., 2015). This is because woodlands are vitally important as habitats for a large part of the world's biodiversity, and for carbon storage, climate regulation and water supply (Thompson, 2011; Hansen et al., 2013). Their ongoing loss, fragmentation and degradation are cause of great concern, especially because of the far-reaching consequences involved (see review by Brockerhoff et al., 2013). Particularly, dry woodlands are fragile ecosystems, with plants and animals especially adapted to thriving under harsh and inhospitable conditions; therefore, dry woodlands and their services have high ecological value (MEA, 2005). Given the many threats dry woodlands face, from both human activity and climate change (Bastin et al., 2017), strategies for their conservation require information on the status of their vegetation. If the challenge is maintaining woodland ecological biodiversity and integrity, it is necessary to assess the condition of this ecosystem through quantifying spatial and temporal changes in vegetation (Lawley et al., 2015). Such assessment should include

✉ Valeria E. Campos
vcampos@unsj-cuim.edu.ar

Viviana N. Fernandez Maldonado
vivifernandezm@unsj-cuim.edu.ar

[1] CIGEOBIO, UNSJ CONICET, Universidad Nacional de San Juan- CUIM, Av. Ignacio de la Roza 590 (O), J5402DCS Rivadavia, San Juan, Argentina

[2] Departamento de Biología, Facultad de Ciencias Exactas, Físicas y Naturales, Universidad Nacional de San Juan, Av. I. de La Roza 590 (O), J5402DCS Rivadavia, San Juan, Argentina

Published online: 24 January 2022

compositional indicators of vegetation, such as species richness, relative abundance, frequency, and proportions of different species. Moreover, structural indicators are measures of the three-dimensional arrangement of vegetation, such as density of the different plant forms, canopy cover, vegetation biomass and foliage density and layering (Noss, 1990). Biomass, directly linked to carbon stocks, is considered a useful indicator of the structural and functional attributes of woodland ecosystems across a wide range of environmental conditions (Brown et al., 1999; Flores-Anderson et al., 2019; Hall et al., 2006). Assessing the performance and accuracy of indicators as a tool for monitoring the condition of vegetation is a key aspect of management and conservation programs (Gaitán et al., 2013; Pyke et al., 2002) and is crucial for establishing future mitigation scenarios under climate change (Latifi et al., 2015).

Two different methods allow monitoring woodland status, field-based and remote sensing data. Field-based data provide indispensable information which can be difficult to acquire across broad spatial extents. The shortcomings of this method lie in inconsistencies between different plot sizes, lack of replication and lack of multiple spatial scales, in its being a costly and time-consuming approach, and difficult to implement in remote areas (Lawley et al., 2015). Remote sensing techniques are considered the most promising approach providing up-to-date information on the status of woodland cover and carbon stocks at different scales (Hall et al., 2006; Smith et al., 2019). This is because remote sensing imagery affords systematic, spatial and temporal data on vegetation attributes (Lawley et al., 2015; Nagendra, 2001) and is increasingly recognised for its applicability to ecological research and to land cover change mapping, and as a proxy for species richness and biodiversity across multiple spatial scales (see review by Bradley et al., 2012; Irisarri et al., 2012). The ability of researchers to accurately measure vegetation characteristics using remotely sensed data varies with the sensor (i.e. spatial, spectral and temporal resolutions, passive or active sensor), background characteristics and vegetation attributes of individual species such as size, shape, aggregation, phenology and physical structure such as canopy cover (Lawley et al., 2015). Particularly, monitoring the spatial and temporal dynamics of dryland ecosystems with remote sensing techniques is defined by unique challenges, such as low vegetation cover, mainly senescent vegetation, high soil background reflectance, high spatial heterogeneity, unpredictable rainfall and frequent periods of drought. Moreover, dryland ecosystems are underrepresented by long-term, continuous field measurements which make it difficult to achieve a robust calibration and proper evaluation of remote sensing data (see review by Smith et al., 2019). Therefore, a high research priority is to define good remote sensing indicators of dry woodland structure and function in order to monitor spatial and temporal vegetation dynamics. These indicators could be a valuable tool for management and conservation of dry woodlands in different regions.

Relationships have been developed between woodland biomass and remote sensing data obtained from Landsat series satellites and backscatter data from Synthetic Aperture Radar (SAR; see review by Hall et al., 2006; Smith et al., 2019). Because Landsat has a large archive of free available data, it has become the primary data source for biomass estimation. For example, the potential variables from Landsat images include individual spectral bands, vegetation indices, transformed images, textural images and fractional images (Lu et al., 2014). Although many vegetation indices have been proposed in previous research, depending on the complexity of woodland stand structure, indices vary in their relationships with biomass (Lu et al., 2014). Nearly all vegetation indices, such as NDVI (Normalised Difference Vegetation Index), are estimators of green and vigorous vegetation, so several studies have used them to map aboveground biomass in boreal, temperate and tropical woodlands (see review by Hall et al., 2006). However, the challenge is capturing information about dry woodland vegetation, which is senescent, with non-photosynthetic tissues for extended periods, and with small leaf areas or leafless (Goirán et al., 2012). Moreover, other challenges posed by these ecosystems are high soil background reflectance, high spatial heterogeneity from plot to ecosystem and regional scales, irregular growing seasons due to unpredictable seasonal rainfall and frequent periods of drought (see review by Smith et al., 2019). The gap in the knowledge of dryland remote sensing should be a top research priority, especially given that drylands cover $\sim$ 41.5% of the Earth's land surface (Bastin et al., 2017) and more than 2 billion people depend on their provision of services (Smith et al., 2019). Studies focused on different remote sensing data and at multi-scale have the potential to significantly advance our current understanding of dryland ecosystems (Smith et al., 2019).

SAR sensors have the advantage to penetrate the canopy; so they are considered the most useful tools for providing measures of woodland vertical structure or stand volume measures. They provide information on the backscattered energy from the illuminated target and can have different wavelengths, and thus different abilities to penetrate woodlands. Depending on the structural and dielectric characteristics of woodland canopies, the relative contribution of volume, surface–volume interactions and surface scattering from forest in the total backscatter signal of an imaging radar can vary (see review by Laurin et al., 2018). SAR imagery can be acquired day and night, in any

weather conditions, so it is particularly useful for monitoring areas where cloud cover is almost permanent and optical images are unusable (Flores-Anderson et al., 2019; Zhu et al., 2012). Therefore, radar data with the capability to penetrate woodland stand structure may provide different performances compared to optical sensor images (see review by Zhao et al., 2016).

Ramorinoa girolae is a woody leguminous tree (Fabaceae) that can reach 10 m tall (Hadad et al., 2014), leafless, though with green stems. It is endemic to central-western Argentina and forms woodland patches whose distribution is fragmented and restricted to mountain slopes and temporary watercourses (Zapata, 2017). This restricted geographical distribution plus its slow growth and low resistance to fire make it a fragile species. Morphologically, this species is characteristic for its reptant stems that could be playing an important role as soil stabilisers, thus reducing wind and water erosion, both these processes being frequent in arid ecosystems. Moreover, its morphological features enable it to maintain different biological interactions with mammals, birds (Campos et al., 2017) and insects (Papú et al., 2015). Therefore, it is of high conservation value due to its provision of biodiversity-related ecosystem services. In our research, we assess whether passive and active remote sensing data are good indicators of vegetation composition and structure in dry *R. girolae*-dominated woodlands on sites with different climate and terrain characteristics. Moreover, because previous studies showed that the relationship between dry woodland composition and structure and different predictors is scale-dependent (Campos et al., 2018, 2020), we assess remote sensing data at multi-scale. Therefore, our objectives were: (1) to quantify on-the-ground vegetation composition and structure in dry *R. girolae*-dominated woodlands on three study sites, using (A) field-based methods and (B) passive and active remotely sensed data at multi-scale and (2) to assess whether the integration of data from different remote sensors allows for a better estimation of field-based measures in dry *R. girolae*-dominated woodlands.

Methods

Study Area

Ramorinoa girolae (Fig. 1) occurs in San Juan, La Rioja and San Luis provinces, mainly in Monte Desert and a portion of Chaco Seco. Our study sites are in the Monte Desert, which occupies 460,000 km^2 of the arid west of Argentina. Thus, the Monte Desert is a region with different climate and edaphic conditions throughout its expanse (Bisigato et al., 2009; Brown et al., 2006). The main communities in the Monte Desert are creosote bush scrub and mesquite woodland. The dry woodlands of *R. girolae* have a fragmented distribution and are restricted to mountain slopes and temporary watercourses (Campos et al., 2016; Hadad et al., 2014; Zapata, 2017). To take into account the high spatial heterogeneity in climatic conditions and terrain features of dry *R. girolae*-dominated woodlands (Table 1), a great challenge in these drylands, we considered three study sites throughout the distribution of the study species. The study sites were (Fig. 2): A Ischigualasto Provincial Park (29° 55′ S, 68° 05′ W) (henceforth Ischigualasto) and its zone of influence, with an area of 62,916 ha. B Valle Fértil Multiple Use Reserve (31° 07′ S, 67° 40′ W) (henceforth Valle Fértil) covering 800,000 ha. C- Private land (31° 44′ S, 67° 59′ W) occupies 4,153 ha.



Fig. 1 Individual of *Ramorinoa girolae* in Ischigualasto Provincial Park

Field Survey

Fieldwork was conducted in wet seasons, from December to March of 2015–2016 and from December to March of 2016–2017, because is the season of the highest productivity (Bisigato et al., 2009). We used three L8 OLI Level-2 Processing Level images (30-m spatial resolution) of the study areas (path/row: 232/81; 231/81 and 232/82) to defined sampling plots. These images, dated February and March (wet season) of 2016 and 2017, were obtained from Earth Explorer USGS (https://earthexplorer.usgs.gov/). We stored these images in the Quantum GIS (Version 3.4.8 "Madeira", 2018), and for each site, we delimited polygons (in logistically accessible areas) of dry *R. girolae*-dominated woodland. The number of plots at each site depended on *R. girolae*-dominated woodland area and its accessibility. Then, using random point tools, we randomly selected field plots within each polygon (Ischigualasto $n = 16$; Valle Fértil $n = 10$; Private land $n = 10$) spaced at

Table 1 Climate and terrain characteristics of the study sites: Ischigualasto, Valle Fértil and private land. Climate data include: maximum temperature, minimum temperature and precipitation accumulation. Terrain data include: altitude, slope and main aspect

Characteristics	Ischigualasto	Valle Fértil	Private land
Maximum temperature (°C)	26.9	26.2	30.0
Minimum temperature (°C)	11.00	10.5	14.1
Precipitation accumulation (mm)	10.00	20.00	27.00
Altitude (m)	1381.06	1709.00	891.00
Slope (degrees)	5.54	10.43	7.51
Main aspect	South	East	Southwest

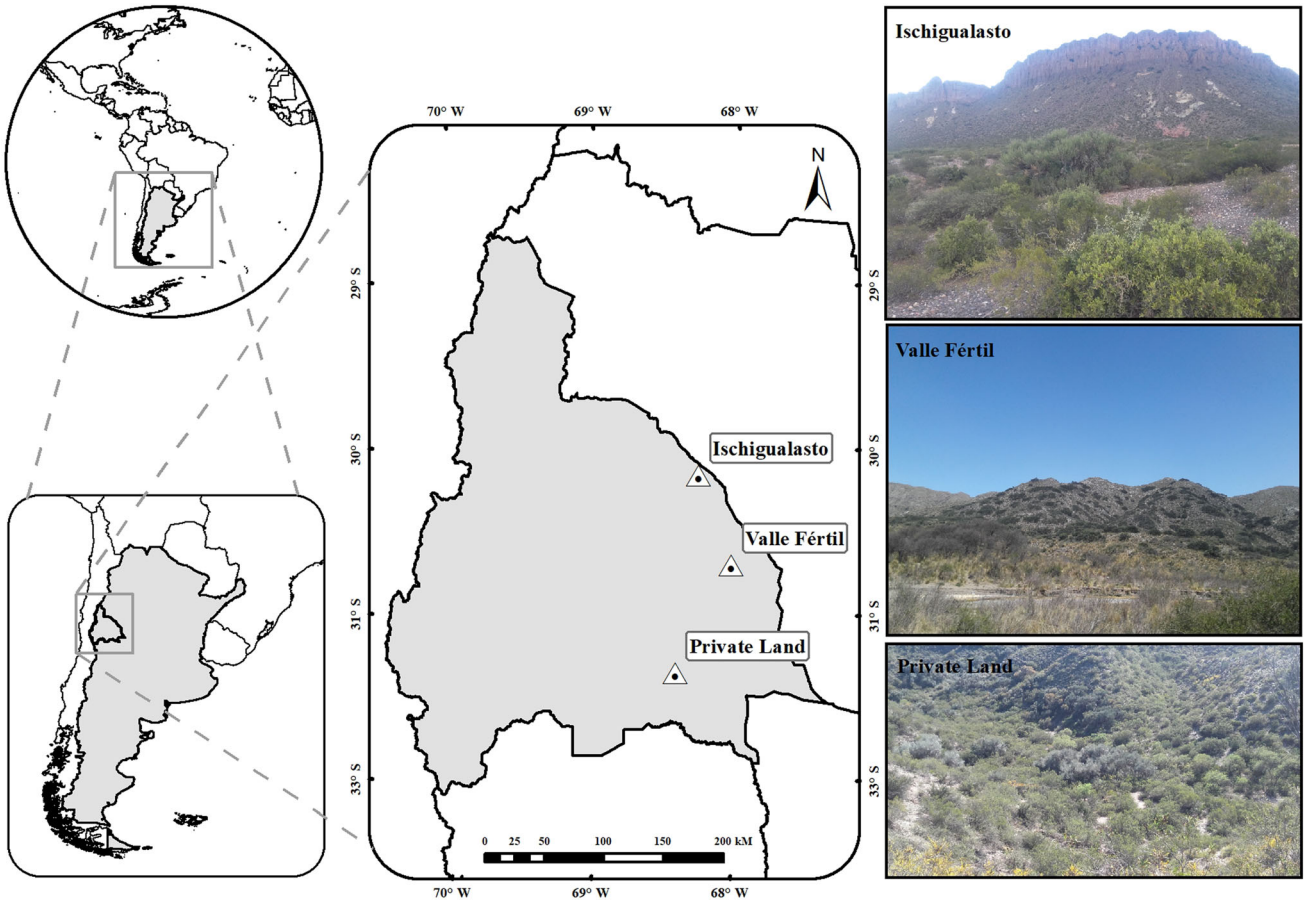


Fig. 2 Map of study sites: Ischigualasto Provincial Park (Ischigualasto), Valle Fértil Multiple Use Reserve (Valle Fértil) and private land, in San Juan province (Argentina)

least 100 m apart. In the field, each plot was 50 × 30 m (0.15 ha stand scale). Inside each plot, we ran four 30-m-long transects separated by 15 m and used the Modified Point Quadrat method (Passera et al., 1983) to determine compositional and structural indicators. Following the Modified Point Quadrat method, we recorded each species that touched the needle every 1 m along each transect, from 0 to 30 m (31 records per transect). Based on this information, we estimated richness (compositional indicator) as number of species touching the needle, and abundance of each species (structural indicator) as number of touches on the needle. To obtain a measure of richness at stand scale, we recorded the tally of species across all subplots. To obtain a measure of abundance of shrubs and trees at stand scale, as a proxy for biomass, we summed up the total number of touches from each shrub/tree species across all subplots (Passera et al., 1983). Also, in each plot we recorded abundance of *R. girolae* and structural measures for each individual: basal diameter of each shaft, tree height and canopy dimensions (largest and smallest diameters). The equivalent basal diameter for each *R. girolae* tree was estimated using the formula employed by Alvarez

et al. (2006), which considers the diameter of each shaft. Because basal diameter, tree height and canopy area (largest * smallest diameters) were strongly correlated ($|\rho| > 0.8$), we considered only the canopy area of *R. girolae*. Also, because we were interested in knowing whether dry *R. girolae* woodland was renewed, we estimated variance in canopy cover in each plot (stand-scale) for the analysis.

Remote Sensing Variables

Climate data for each site (Table 1) were obtained from TerraClimate with monthly temporal resolution and a ~ 4-km spatial resolution. We considered a period from 1990 to 2020 (Abatzoglou et al., 2018). Terrain data, i.e. altitude, slope and aspect, for each site (Table 1) were obtained from Shuttle Radar Topography Mission (SRTM 30 m resolution, from Earth Explorer USGS). We calculated the mean of each variable from the values of the plots (Table 1).

Passive Remote Sensing Data

In drylands with generally low and senescent vegetation cover, the soil background tends to significantly influence green indexes, such as NDVI (Normalised Difference Vegetation Index) which is a good estimator of green and vigorous vegetation but shows limited success in measuring senescent and leafless vegetation (see review by Smith et al., 2019). Therefore, from the three L8 OLIs of the study sites, we estimated two vegetation indices EVI (Enhanced Vegetation Index, Huete et al., 2002) and SATVI (Soil Adjusted Total Vegetation Index, Marsett et al., 2006). EVI is responsive to canopy structural variations, including leaf area index (LAI), canopy type, plant physiognomy and canopy architecture (Gao et al., 2000). This index improves upon the detection of canopy biophysical parameters and can be supplemented with a green vegetation index such as SATVI, which is sensitive to both green and senescent vegetation, and includes a parameter (L) that minimises the effects of soil background on the vegetation signal. Therefore, this is a good proxy for vegetation cover in desert areas (Campos et al., 2015, 2018; Goirán et al., 2012). Huete (1988) recommended $L = 0.5$ for intermediate vegetation densities, so we considered this value for dry *R. girolae*-dominated woodlands. We used Quantum GIS for optical image processing.

Active Remote Sensing Data

Sentinel-1A (band C) interferometric wide swath data (ground range detected—GRD—products) with an observation date (February 2016—wet season) coincidental with field measurement were downloaded from Alaska Satellite Facility (https://www.asf.alaska.edu/). We considered the C-band because shrubs are the predominant vegetation; moreover, our target species has a semi-decumbent growth habit since secondary branches grow horizontally or downwards, and sometimes, as decumbent because of reaching to the ground (Pasiecznik et al., 2001). This growth habit is probably due to the high density of the wood (Kiesling, 1994) that pulls the heavy branches down. SAR systems are characterised by the direction (with respect to the electrical field vector) of transmitted and return signals. Sentinel-1A data were in the dual-polarisation of VV (co-polarisation) and VH (cross-polarisation). The radiometric calibration was expressed in Sigma-nought (σ^0_{VV} σ^0_{VH}) backscatter coefficient intensity (original scale). These products were terrain corrected using one-arc second SRTM data (30 m) from Earth Explorer USGS. The Sentinel data were resampled from 10 m × 10 m cell size to 30 m × 30 m, so all the data had the same cell size. We did not perform filtering for speckle noise reduction. We processed all images with SNAP 6.0 (http://step.esa.int/main/download/).

For all remote sensing data obtained from optical (i.e. EVI and SATVI) and SAR backscatter values (i.e. for VV and VH), we estimated standard deviation (SD) using 3 × 3, 5 × 5 and 7 × 7 moving windows, i.e. the pixel values within a moving window were used to calculate a statistic that was assigned to the central pixel. All remote sensing data were finally stored as separate layers in the GIS and were extracted for each sampling field plot using Quantum GIS.

Statistical Analysis

Considering the variables shown in Table 2, we employed generalised linear models (GLMs) for each study site. For each response variable: richness, biomass of shrubs and trees and abundance of *R. girolae*, we employed GLMs with Poisson error distribution. Because some models exhibited overdispersion, we adjusted a negative binomial distribution (Zuur et al., 2009). We applied logarithmic transformations to variance in canopy cover of *R. girolae* because model residuals were not normally distributed (Zar, 1999). We fitted models with optical remote sensing data (i.e. EVI and SATVI) at each scale (i.e. 3 × 3, 5 × 5 and 7 × 7 moving windows) for each response variable separately (single-sensor models). In the same way, we fitted models with SAR backscatter data (i.e. for VV co-polarisation and VH cross-polarisation) at each scale (i.e. 3 × 3, 5 × 5 and 7 × 7 moving windows) for each response variable separately (single-sensor models). All fixed variables were standardised by z-scores prior to

Table 2 Description of response and predictor variables considered in models to determine vegetation composition and structure in *R. girolae*-dominated woodlands at different scales

Variable	Description	In models	Variable type
Species richness	Total number of species per plot	Response	Discrete
Shrubs biomass	Sum of total touches of shrubs per plot	Response	Discrete
Trees biomass	Sum of total touches of trees per plot	Response	Discrete
Abundance of *R. girolae*	Total number of *R. girolae* per plot	Response	Discrete
Canopy variance of *R. girolae*	Variance of canopy area for all *R. girolae* recorded per plot	Response	Continuous
EVI (Enhanced vegetation index)	Standard deviation	Predictor	Continuous
SATVI (Soil adjusted total vegetation index)	at 3 × 3, 5 × 5 and 7 × 7	Predictor	Continuous
VV co-polarisation	Moving windows	Predictor	Continuous
VH cross-polarisation		Predictor	Continuous

analysis. For the last objective, we considered the significant variables from single-sensor models to fit a multi-sensor model at each study site and moving window. We only inform the multi-sensor models when these have variables from different remote sensing data. For each full model, a backward elimination procedure was used to remove insignificant variables without losing important information (significance level $p < 0.05$) and to obtain the minimal adequate model (Crawley, 2007). We estimated a pseudo-R^2 from deviance values of the best models (Zuur et al., 2009). To check for spatial autocorrelation among sampling points, we fitted semivariograms with the Pearson residuals of the regression models (Zuur et al., 2009). We found no evidence of spatial dependence affecting the models. All statistical analyses and figures were conducted using R (R Core Team, 2019) using the following packages: "geoR" (Ribeiro and Diggle, 2016), "MASS" (Venables & Ripley, 2002), "GGally" (Schloerke et al., 2020).

Results

The sampling of plants recorded at stand scale in dry *R. girolae*-dominated woodlands showed the highest species richness, shrub and tree biomass in private land, whereas the highest abundance of *R. girolae* was found in Valle Fértil, and the highest variance in canopy cover of *R. girolae* in Ischigualasto (Table 3). The lowest records for shrub biomass and variance in canopy cover of *R. girolae* were found in Valle Fértil, and the lowest records for species richness, tree biomass and abundance of *R. girolae* were found in Ischigualasto (Table 3). The height of *R. girolae* at stand scale was 2.70 ± 0.17 m (mean ± SE; min = 0.07, max = 8.50 m) for Ischigualasto; 1.81 ± 0.08 m (min = 0.20, max = 5.10 m) for Valle Fértil, and 3.88 ± 0.19 m (min = 0.82 and max = 8.00 m) for private land. The proportion of adult *R. girolae* trees (with equivalent basal diameter larger than 7.5 cm, Alvarez et al., 2006) was 87% for Ischigualasto, 50% for Valle Fértil and 86% for private land. Appendices 1 and 2 show SD of EVI, SATVI and backscatter values in VH and VV polarisations. The highest and lowest range values of SD for EVI were found in Valle Fértil and private land, respectively. Conversely, the highest and lowest range values of SD for SATVI were found in private land and Valle Fértil, respectively. Regarding backscatter values in VH and VV polarisations, we found the highest and lowest range values of SD in Ischigualasto and private land, respectively.

Neither passive nor active remote sensing data explained the richness found on the different study sites (Tables 4, 5 and 6). Shrub biomass in the single-sensor models of Ischigualasto was explained by a positive relationship with SD of EVI (7 × 7 moving window, Table 4), negative with SD of VV co-polarisation and positive with SD of VH cross-polarisation at all moving windows (Table 4). Tree biomass, in the single-sensor models, was explained by a positive relationship with SD of VV co-polarisation at all scales (Table 4). Abundance of *R. girolae*, in the single-sensor models, was negatively related to SD of SATVI (3 × 3 moving window) and SD of EVI (5 × 5 moving window), and positively to SD of VV co-polarisation (at all scales, Table 4). The multi-sensor models that included SD of SATVI and SD of VV co-polarisation (3 × 3 moving window) showed a higher explained variance than single-sensor models (Fig. 3, Appendix 3). Regarding variance in canopy cover of *R. girolae* in the single-sensor models, it had a positive relationship with SD of EVI (3 × 3 and 5 × 5 moving windows) and SD of SATVI (7 × 7 moving

Table 3 Summary statistic for field-based data at stand scale. Shown here are mean (± SE), minimum and maximum values of variables

Field-based data	Statistics value	Ischigualasto Provincial Park	Valle Fértil Multiple Use Reserve	private land
Richness	Mean ± SE	11.00 ± 0.76	12.60 ± 0.81	14.60 ± 0.87
	Min–Max	7.00–19.00	9.00–15.00	10.00–19.00
Shrubs biomass	Mean ± SE	147.56 ± 20.16	39.30 ± 4.31	241.70 ± 25.86
	Min–Max	36.00–309.00	17.00–56.00	143–351.00
Trees biomass	mean ± SE	39.88 ± 6.74	48.80 ± 16.86	61.40 ± 11.94
	Min–Max	7.00–113.00	0.00–140.00	0.00–137.00
Abundance of *R. girolae*	Mean ± SE	5.38 ± 0.75	24.00 ± 7.16	6.80 ± 1.31
	Min–Max	2.00–12.00	6.00–86.00	1.00–14.00
Canopy variance of *R. girolae*	Mean ± SE	8608.36 ± 4656.35	853.11 ± 285.43	3637.55 ± 2135.43
	Min–Max	62.49–72,200.00	96.00–2761.67	0.00–22,408.39

window, Table 4). Active remote sensing data (i.e. SD of VV and VH) explained up to 55% of the variability in variance of shrubs biomass, these being the best remote sensing data explaining field-based data for this study site.

In Valle Fértil, the biomass of shrubs in single-sensor model*s* had a negative relationship with SD of SATVI (3 × 3 and 5 × 5 moving windows) and SD of VH cross-polarisation (3 × 3 moving window), while tree biomass was explained by a negative relationship with SD of VV co-polarisation (3 × 3 and 7 × 7 moving windows, Table 5) and positive with SD of VH cross-polarisation (3 × 3 moving window). Regarding abundance of *R. girolae,* it was negatively related to SD of VH cross-polarisation (3 × 3 and 7 × 7 moving windows), and canopy variance had a positive relationship with SD of SATVI (7 × 7 moving window, Table 5). In the single-sensor models from Valle Fértil (5 × 5 moving window), active remote sensing data (i.e. SD of VV and VH polarisation) explained up to 64% of the variability in tree biomass in dry *R. girolae*-dominated woodlands, these being the best models explaining field-based data. In the multi-sensor models (3 × 3 moving window) that included SD of SATVI and VH cross-polarisation, the explained variability for shrubs biomass was up to 46% (Fig. 4, Appendix 3).

In the private land, the biomass of shrubs was explained by a negative relationship with SD of EVI at all scales, SD of VH cross-polarisation (3 × 3 moving window) and a positive relationship with SD of SATVI at the 7 × 7 moving window (Table 6). In the multi-sensor models (3 × 3 moving window) that included SD of EVI and VH cross-polarisation, the explained variability was up to 59% (Fig. 5, Appendix 3). Tree biomass was explained by a positive relationship with SD of SATVI (5 × 5 and 7 × 7 moving windows) and negative with SD of EVI (5 × 5 and 7 × 7 moving windows, Table 6). Moreover, it was explained by a negative relationship with SD of VV co-polarisation at all scales and positive with SD of VH at 7 × 7 moving window (Table 6). Neither abundance nor variance in canopy cover of *R. girolae* was explained by passive or active remote sensing data (Table 6). At this study site, single-sensor model with active remote sensing data (i.e. SD of VV co-polarisation and VH cross-polarisation) explained up to 83% of the variability in tree biomass in dry *R. girolae*-dominated woodlands. Nevertheless, in multi-sensor models (7 × 7 scale), the variables SD of EVI and SATVI and SD of VV and VH polarisation explained 90% of the variability in tree biomass (Fig. 6, Appendix 3).

Discussion

The results of this approach to assessing compositional and structural indicators of vegetation condition at different scales show that passive and active remote sensing data were good indicators of almost all field-based data (i.e. shrub biomass, tree biomass, abundance and variance in canopy cover of *R. girolae*) recorded at stand scale. The multi-sensor models were better than single-sensor models to explain the attributes of these woodlands, except for the canopy variance of *R. girolae* (single-sensor model that included EVI). Considering the best models, we found that EVI and VH cross-polarisation explained shrubs biomass, and the SATVI with VV co-polarisation explained the abundance of *R. girolae*. Moreover, both green indexes (i.e. EVI and SATVI) and polarisations (i.e. VV and VH) explained the biomass of the trees. Richness was the only field-based data not related to remote sensing data, either passive or active, at any study site. These results disagree with Rocchini et al. (2004) and Campos et al. (2018), who found a scale-dependent relationship between data obtained from remote sensors and species richness. Probably, richness in *R. girolae*-dominated woodland could be

Table 4 Results of single-sensor models for Ischigualasto Provincial Park, after backward elimination procedures, for field-based data (richness, shrub and tree biomass, abundance and variance in canopy cover of *R. girolae*)

Field-based data	Moving window	Source image	Predictor/s	Estimate ± SE	*p*-Value	pseudo-R^2
Richness	3 × 3	L8 OLI	SATVI	0.04 ± 0.08	0.61	–
		Sentinel-1A	VV	0.07 ± 0.07	0.35	–
	5 × 5	L8 OLI	EVI	− 0.02 ± 0.08	0.80	–
		Sentinel-1A	VV	0.08 ± 0.07	0.29	–
	7 × 7	L8 OLI	EVI	− 0.08 ± 0.08	0.34	–
		Sentinel-1A	VV	0.09 ± 0.07	0.23	–
Shrubs biomass	3 × 3	L8 OLI	EVI	0.19 ± 0.13	0.14	–
		Sentinel-1A	VV	− 0.57 ± 0.18	**	47.68
		Sentinel-1A	VH	0.69 ± 0.18	***	
	5 × 5	L8 OLI	EVI	0.19 ± 0.13	0.14	–
		Sentinel-1A	VV	− 0.40 ± 0.13	**	51.88
		Sentinel-1A	VH	0.51 ± 0.13	***	
	7 × 7	L8 OLI	EVI	0.25 ± 0.12	*	23.11
		Sentinel-1A	VV	− 0.49 ± 0.13	***	55.07
		Sentinel-1A	VH	0.57 ± 0.13	***	
Trees biomass	3 × 3	L8 OLI	SATVI	− 0.18 ± 0.17	0.31	–
		Sentinel-1A	VV	0.31 ± 0.15	*	24.57
	5 × 5	L8 OLI	SATVI	− 0.19 ± 0.17	0.25	–
		Sentinel-1A	VV	0.30 ± 0.15	*	22.92
	7 × 7	L8 OLI	SATVI	− 0.18 ± 0.17	0.30	–
		Sentinel-1A	VV	0.33 ± 0.15	*	26.52
Abundance of *R. girolae*	3 × 3	L8 OLI	SATVI	− 0.34 ± 0.14	*	30.99
		Sentinel-1A	VV	0.28 ± 0.09	**	37.15
	5 × 5	L8 OLI	EVI	− 0.34 ± 0.15	*	29.91
		Sentinel-1A	VV	0.28 ± 0.09	**	35.87
	7 × 7	L8 OLI	EVI	− 0.24 ± 0.15	0.11	–
		Sentinel-1A	VV	0.26 ± 0.10	*	27.52
Canopy variance of *R. girolae*	3 × 3	L8 OLI	EVI	0.19 ± 0.06	**	42.37
		Sentinel-1A	VV	− 0.33 ± 0.53	0.54	–
	5 × 5	L8 OLI	EVI	1.42 ± 0.38	**	49.59
		Sentinel-1A	VH	0.52 ± 0.52	0.34	–
	7 × 7	L8 OLI	SATVI	1.32 ± 0.41	**	42.69
		Sentinel-1A	VV	− 0.40 ± 0.53	0.46	–

on *R. girolae*-dominated woodlands, considering standard deviation (SD) of remote sensing data (i.e. SATVI, EVI, VV co-polarisation and VH cross-polarisation) as different predictor variables. Shown here are parameter estimates (± SE), *p*-values for significance (* = $p \leq 0.05$; ** = $p < 0.01$, *** = $p < 0.001$) and pseudo-R^2 for models

related to texture measures of SATVI, proxies for net primary productivity, as was reported by Campos et al. (2018) for *Prosopis flexuosa*-dominated woodland or to another green index not considered in this research. Different mechanisms have been proposed to explain how species richness responds to variation in productivity, particularly, in *Prosopis flexuosa*-dominated woodland which was explained, in less, by productivity and mainly by the abundance of trees (Campos et al., 2020). The positive effect of facilitation provided by woody species is crucial in dry ecosystems (Cesca et al., 2012).

Climate, soil, topography and disturbance are recognised as the most important factors influencing the organisation and distribution of plant communities, the abundance and growth of tree species and the regulation of various ecosystem processes, at both temporal and spatial scales (see review by Piraino et al., 2015). We found high heterogeneity among our study sites regarding climatic and

Table 5 Results of single-sensor models for Valle Fértil Multiple Use Reserve, after backward elimination procedures, for field-based data (richness, shrub and tree biomass, abundance and variance in canopy cover of *R. girolae*)

Field-based data	Moving window	Source image	Predictor/s	Estimate ± SE	*p*-value	pseudo-R^2
Richness	3 × 3	L8 OLI	SATVI	− 0.09 ± 0.09	0.38	–
		Sentinel-1A	VH	− 0.15 ± 0.11	0.16	–
	5 × 5	L8 OLI	SATVI	− 0.07 ± 0.10	0.48	–
		Sentinel-1A	VH	− 0.12 ± 0.11	0.25	–
	7 × 7	L8 OLI	EVI	0.06 ± 0.09	0.54	–
		Sentinel-1A	VH	− 0.12 ± 0.10	0.26	–
Shrubs biomass	3 × 3	L8 OLI	SATVI	− 0.21 ± 0.10	*	26.04
		Sentinel-1A	VH	− 0.21 ± 0.1	*	27.43
	5 × 5	L8 OLI	SATVI	− 0.23 ± 0.10	*	31.39
		Sentinel-1A	VV	− 0.20 ± 0.11	0.07	24.22
	7 × 7	L8 OLI	SATVI	− 0.09 ± 0.11	0.41	–
		Sentinel-1A	VV	− 0.18 ± 0.11	0.09	–
Trees biomass	3 × 3	L8 OLI	EVI	− 0.15 ± 0.49	0.76	–
		Sentinel-1A	VV	− 3.82 ± 1.35	*	63.61
		Sentinel-1A	VH	1.45 ± 0.63	**	
	5 × 5	L8 OLI	EVI	0.29 ± 0.48	0.55	–
		Sentinel-1A	VV	− 2.33 ± 1.38	0.09	–
	7 × 7	L8 OLI	SATVI	0.60 ± 0.47	0.20	–
		Sentinel-1A	VV	− 1.58 ± 0.62	*	19.38
Abundance of *R. girolae*	3 × 3	L8 OLI	SATVI	− 0.17 ± 0.23	0.46	–
		Sentinel-1A	VH	− 0.44 ± 0.23	*	22.52
	5 × 5	L8 OLI	EVI	− 0.27 ± 0.22	0.22	–
		Sentinel-1A	VV	− 0.45 ± 0.25	0.06	–
	7 × 7	L8 OLI	SATVI	− 0.12 ± 0.23	0.61	–
		Sentinel-1A	VH	− 0.45 ± 0.22	*	27.62
Canopy variance of *R. girolae*	3 × 3	L8 OLI	EVI	− 0.26 ± 0.41	0.55	–
		Sentinel-1A	VV	− 0.39 ± 0.40	0.35	–
	5 × 5	L8 OLI	EVI	0.45 ± 0.39	0.28	–
		Sentinel-1A	VV	− 0.05 ± 0.07	0.47	–
	7 × 7	L8 OLI	SATVI	0.75 ± 0.33	*	39.92
		Sentinel-1A	VV	− 0.31 ± 0.41	0.46	–

on *R. girolae* -dominated woodlands, considering standard deviation (SD) of remote sensing data (i.e. SATVI, EVI, VV co-polarisation and VH cross-polarisation) as different predictor variables. Shown here are parameter estimates (± SE), *p*-values for significance (* = $p \leq 0.05$; ** = $p < 0.01$, *** = $p < 0.001$) and pseudo-R^2 for models

topographic features. There is a N-S precipitation gradient, Ischigualasto being the site with the lowest values for precipitation, and regarding topographic features, Valle Fértil is the site with the highest mean values for altitude and slope. The aridity conditions and topographic features of these environments are limiting for the growth and development of vegetation, and the cause of development of morpho-functional adaptations in the species inhabiting these dry woodlands (Zapata, 2017). In addition, local and temporal variations can result in differential dynamics of vegetation communities for each woodland site (Hadad et al., 2014; Zapata, 2017).

Shrub biomass was explained by passive (57% in private land) and active (55% in Ischigualasto) remote sensing data. Increases in shrub biomass were related to a decrease in SD of EVI (at all scales) and an increase in SD of SATVI (7 × 7 moving window); moreover, they were related to a decrease in SD of VV and an increase in SD of VH polarisation (at all scales). In Valle Fértil, shrubs biomass was better explained by the multi-sensor model at the 3 × 3 moving window (46%) than by single-sensor models (26% passive and 27% active). When comparing our study sites, private land was the site with the highest shrub biomass; probably EVI, which is responsive to

Table 6 Results of single-sensor models for private land, after backward elimination procedures, for field-based data (richness, shrub and tree biomass, abundance and variance in canopy cover of *R. girolae*) on

Field-based data	Moving window	Source image	Predictor/s	Estimate ± SE	*p*-value	pseudo-R^2
Richness	3 × 3	L8 OLI	SATVI	− 0.02 ± 0.09	0.74	–
		Sentinel-1A	VV	0.12 ± 0.10	0.24	–
	5 × 5	L8 OLI	EVI	− 0.03 ± 0.09	0.77	–
		Sentinel-1A	VV	− 0.12 ± 0.10	0.22	–
	7 × 7	L8 OLI	SATVI	− 0.03 ± 0.09	0.72	–
		Sentinel-1A	VV	− 0.12 ± 0.10	0.24	–
Shrubs biomass	3 × 3	L8 OLI	EVI	− 0.19 ± 0.09	*	28.76
		Sentinel-1A	VH	− 0.20 ± 0.09	*	32.16
	5 × 5	L8 OLI	EVI	− 0.19 ± 0.09	*	32.87
		Sentinel-1A	VH	− 0.03 ± 0.11	0.79	–
	7 × 7	L8 OLI	EVI	− 0.46 ± 0.13	***	56.64
		L8 OLI	SATVI	0.34 ± 0.13	**	
		Sentinel-1A	VH	− 0.09 ± 0.10	0.40	–
Trees biomass	3 × 3	L8 OLI	SATVI	− 0.12 ± 0.29	0.69	–
		Sentinel-1A	VV	− 1.30 ± 0.31	***	51.86
	5 × 5	L8 OLI	EVI	− 0.36 ± 0.06	***	18.92
		L8 OLI	SATVI	0.13 ± 0.06	*	
		Sentinel-1A	VV	− 1.89 ± 0.61	**	77.53
	7 × 7	L8 OLI	EVI	− 0.79 ± 0.09	***	38.70
		L8 OLI	SATVI	0.60 ± 0.09	***	
		Sentinel-1A	VV	− 2.16 ± 0.61	***	82.99
		Sentinel-1A	VH	0.47 ± 0.16	**	
Abundance of *R. girolae*	3 × 3	L8 OLI	EVI	− 0.31 ± 0.19	0.09	–
		Sentinel-1A	VV	− 0.47 ± 0.24	0.06	–
	5 × 5	L8 OLI	SATVI	− 0.21 ± 0.19	0.29	–
		Sentinel-1A	VV	− 0.33 ± 0.23	0.16	–
	7 × 7	L8 OLI	SATVI	− 0.22 ± 0.19	0.25	–
		Sentinel-1A	VV	− 0.34 ± 0.23	0.15	–
Canopy variance of *R. girolae*	3 × 3	L8 OLI	EVI	0.33 ± 0.69	0.65	–
		Sentinel-1A	VH	− 0.15 ± 0.52	0.78	–
	5 × 5	L8 OLI	SATVI	0.45 ± 0.53	0.42	–
		Sentinel-1A	VV	0.19 ± 0.52	0.73	–
	7 × 7	L8 OLI	EVI	0.37 ± 0.54	0.52	–
		Sentinel-1A	VV	0.14 ± 0.53	0.79	–

R. girolae -dominated woodlands, considering standard deviation (SD) of remote sensing data (i.e. SATVI, EVI, VV co-polarisation and VH cross-polarisation) as different predictor variables. Shown here are parameter estimates (± SE), *p*-values for significance (* = $p \leq 0.05$; ** = $p < 0.01$, *** = $p < 0.001$) and pseudo-R^2 for models

structural variations and plant physiognomy, captured this woodland as homogeneous patches of vegetation. Instead, the green index SATVI, which is mainly sensitive to both green and senescent vegetation, showed an increase in its variation probably due to the occurrence of islands of vegetation captured at our largest study scale. Our results are in accord with the revision by Bisigato et al. (2009), who reported that plant patches dominated by shrubs and/or trees are key structures throughout the Monte Desert. However, contrary results were reported by other authors, who found an inverse relationship between shrub abundance and texture measures of heterogeneity (range and entropy) at 3 × 3 and 5 × 5 scales in *P. flexuosa*-dominated woodlands (Campos et al., 2018). Probably, the relationship between shrubs biomass and remote sensing data is scale-dependent. The C-band of SAR data is

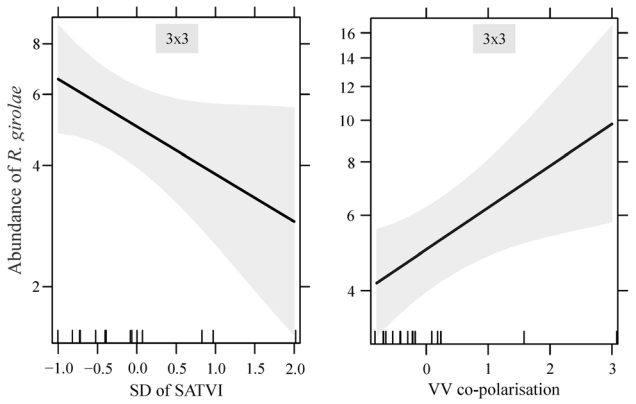


Fig. 3 Multi-sensor model for Ischigualasto Provincial Park, for abundance of *R. girolae*, considering standard deviation (SD) of remote sensing data from SATVI and VV co-polarisation as predictor variables at 3 × 3 moving window. The black line represents the predicted values and the grey area the confidence intervals

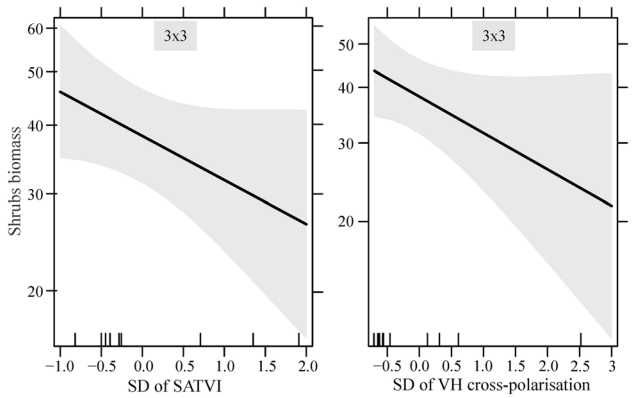


Fig. 4 Multi-sensor model for the Valle Fértil Multiple Use Reserve, for shrubs biomass of *R. girolae*-dominated woodlands, considering standard deviation (SD) of remote sensing data from SATVI and VH cross-polarisation as predictor variables at 3 × 3 moving window. The black line represents the predicted values and the grey area the confidence intervals

typically applied to monitoring areas with low-to-moderate vegetation (Flores-Anderson et al., 2019). Vegetation canopies belong to the category of volume scatterers because the signals bounce multiple times as they propagate through vegetation structure (Flores-Anderson et al., 2019). This band provides data on backscattering mainly from leaves and needle leaves (Laurin et al., 2018). An inverse relationship of shrub biomass with SD of VH polarisation could be because private land has the highest shrub biomass, captured by SAR as homogeneous patches of vegetation at 3 × 3 scale. However, in Ischigualasto the relationship with SD of VH polarisation was positive at all scales, probably due to heterogeneous distribution of vegetation patches. Because of the sensitivity of the cross-polarised signature to the multiple scattering that occurs in

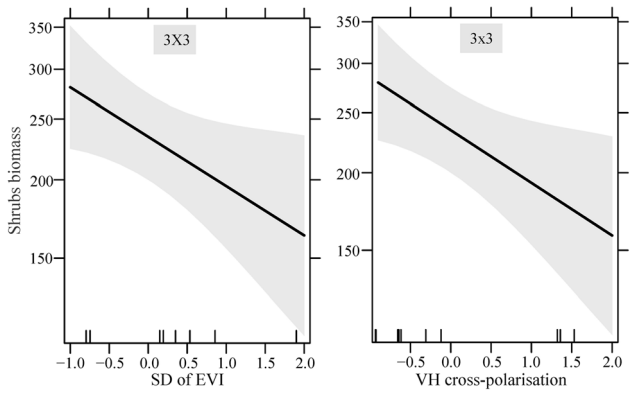


Fig. 5 Multi-sensor model for the private land, for shrubs biomass of *R. girolae*-dominated woodlands, considering standard deviation (SD) of remote sensing data from EVI and VH cross-polarisation as predictor variables at 3 × 3 moving window. The black line represents the predicted values and the grey area the confidence intervals

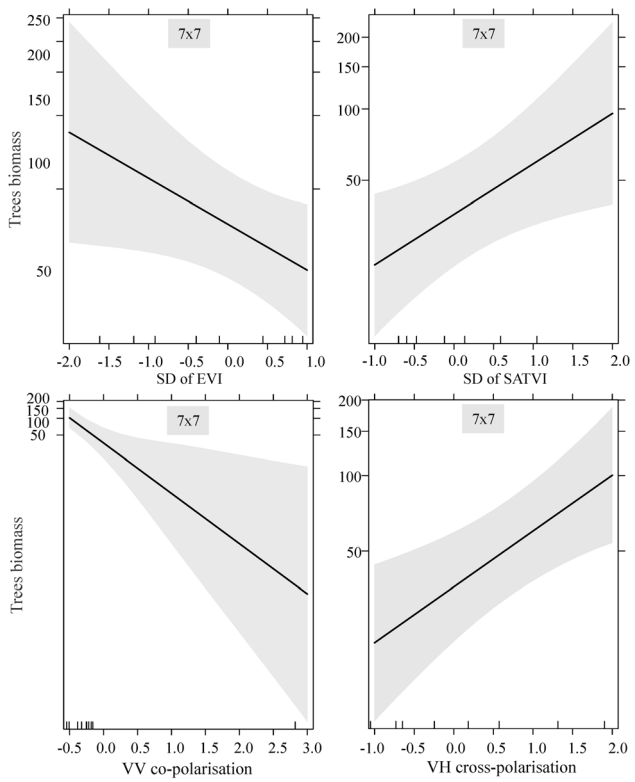


Fig. 6 Multi-sensor model for the private land, for trees biomass of *R. girolae*-dominated woodlands, considering standard deviation (SD) of remote sensing data from EVI, SATVI, VV and VH polarisations as predictor variables at 7 × 7 moving window. The black line represents the predicted values and the grey area the confidence intervals

vegetated environments, this polarisation is the most often used for characterising forest structure (Flores-Anderson et al., 2019).

Tree biomass was mainly explained by active remote sensing data. The SD of VV and VH polarisation explained up to 83% of the variability in tree biomass in private land and up to 64% in Valle Fértil. In private land, however, tree biomass was better explained by the multi-sensor model at the 7 × 7 moving window (90% of the variability), which includes SD of VV and VH polarisation and SD of EVI and SATVI. The private land has the highest tree biomass; therefore, the variation in co-polarisation and cross-polarisation could be due to variation in the signal produced by multiple bounces on trees of different species. This is consistent with previous studies where, at higher aboveground biomass, the contribution of volume or multiple scattering from vegetation canopy to the backscattering coefficient dominates (Crabbe et al., 2019). Moreover, passive remote sensing data were included in the best multi-sensor model, capturing this woodland as homogenous structurally patches of vegetation. Plant patches dominated by shrubs and/or trees are associated with fertility islands, which are formed as a result of abiotic and biotic processes (see review by Bisigato et al., 2009). Identifying good indicators of structural attributes of vegetation patches in dry woodland is a useful tool for assessing and monitoring the condition of vegetation in this dry ecosystem, which will contribute to its management and conservation.

Important to highlight is the great heterogeneity and spatial irregularity in the distribution of *R. girolae* (Zapata, 2017). *R. girolae* abundance showed dissimilar values in the different woodlands studied. Ischigualasto, which has the lowest abundance of *R. girolae* but the highest percentage of *R. girolae* adult trees (87%), showed a negative relationship with SD of EVI and SATVI (31% of explained variability), probably because these woodlands were captured by passive remote sensors as homogeneous mature woodland. Moreover, the variation in VV polarisation explained up to 37% of the variability in *R. girolae* abundance. The backscatter from co-polarisation (VV, HH) is typically stronger for surface scattering components, whereas cross-polarisation (VH or HV) is associated with measuring volume scattering. For this reason, VH or the VV/VH ratio is used for biomass applications, forest degradation tracking and identifying changes from volumes to surfaces (Flores-Anderson et al., 2019). However, probably the relationship between SD of VV polarisation with the abundance of R. girolae is due to its particular morphology, a species without leaves and with upright stems or with secondary stems that grew up down or lie near the ground. When significant variables of single-sensor models (i.e. SD of EVI, SATVI and VV co-polarisation) were included in multi-sensor models, there was an increase in the explained variance (up to 54%), at the 3 × 3 moving window. According to Zapata (2017), if we consider the spatial heterogeneity of dry *R. girolae*-dominated woodlands, we can find stands with isolated individuals scattered over the space, stands with uniformly distributed individuals or stands with individuals associated with temporary watercourses. The penetration depth of a SAR signal into a vegetation canopy is influenced by the density of this canopy (Flores-Anderson et al., 2019); therefore, probably the woodland stands in Ischigualasto have isolated adult individuals scattered over the space, which allows for high variation in VV polarisation. The highest abundance of *R. girolae* was for Valle Fértil, probably with uniformly distributed individuals that were captured by active remote sensing data (28% of explained variability), showing an inverse relationship with SD of VH polarisation. In previous studies, backscatter values for cross-polarisation were observed to be more responsive to variation in aboveground biomass than values for co-polarisation (see review by Crabbe et al., 2019).

In Ischigualasto, the data from passive remote sensors (i.e. SD of EVI and SATVI) explained up to 49% of the variability in *R. girolae* canopy, at all scales, while up to 39% of this variability was explained by SD of SATVI in Valle Fértil. The highest variance in canopy cover of *R. girolae* was found in Ischigualasto and was captured as higher variability by EVI and SATVI. Similar results were reported by Campos et al. (2018) for *P. flexuosa*-dominated woodlands, where canopy area was related to SATVI measures of texture heterogeneity at the 5 × 5 moving window. Regarding Valle Fértil, the lowest canopy variance was recorded at stand scale probably because this woodland had only 50% of adult trees, and the rest were seedlings (33%, individuals with DAB < 7.5 cm) and saplings (17%, individuals with DAB < 5 cm). Considering that the average diameter of *R. girolae* increases by 2 mm per year (Zapata, 2017), woodlands with a high number of individuals in lower diameter classes could have been having higher rates of regeneration over the last decades. Moreover, Valle Fértil is the site with the lowest annual mean temperature, which could probably be favouring the germinative power of seeds, which need a period of low temperatures before germination (Zapata, 2017). On the other hand, the main aspect of this site is east, which implies a higher intensity of solar rays compared to the other study sites, where the main aspect is south. These are the only woodlands reported to have high percentage of seedlings and saplings, while other sites of dry *R. girolae*-dominated woodlands have a high percentage of adult individuals (Hadad et al., 2014; Zapata, 2017) which implies high risk of population decline in the future.

Native vegetation is widely recognised as an important resource that provides vital ecosystem services that benefit man, flora and fauna (Lawley et al., 2015). In the Monte Desert, the presence of woody species is a fundamental

determinant of ecosystem processes for they produce changes in microclimate and soil properties through nutrient accumulation. These conditions favour establishment of plant species, increasing the system's total biodiversity, and thereby facilitating biological interactions and reducing the eroding effects of wind and water (Campos et al., 2017; Cesca et al., 2012; Rossi & Villagra, 2003; Villagra, 2000). Despite the high ecological value of these woodlands, there are significant deficiencies in the basic knowledge of their composition and structure. Remote sensing techniques are considered the most promising approach for providing up-to-date information about vegetation at different scales. However, due to the previously summarised challenges, our current understanding of dry woodland dynamics remains limited, so we have yet to reach the full potential of dryland remote sensing data (Smith et al., 2019). The synergy of passive and active remote sensing data and the combination of different spatial resolutions improve studies of vegetation features (Mendes et al., 2019), as was found for some compositional and structural indicators evaluated in this research. However, there is little information about how the synergy and combination of different data can contribute to studies of structure and function of dry woodland vegetation. This work expands our understanding of the relationship of field-based data with both passive and active remotely sensed data, providing evidence that they could be used as a proxy for vegetation structure. Therefore, our findings will contribute to identifying sites with high shrub and tree biomass, and high abundance of *R. girolae*. Moreover, data obtained from passive and active remote sensors were related to variability in the canopy area of *R. girolae* and could therefore be a useful tool for ascertaining whether the woodland is renewed. Measuring the structural heterogeneity of woodlands allows assessing their condition and dynamics, regeneration patterns, microclimate variation, habitat availability for wildlife and economic aspects (see review by Zenner & Hibbs, 2000). Our findings would help identify sites in need of development of conservation strategies for dry *R. girolae*-dominated woodlands.

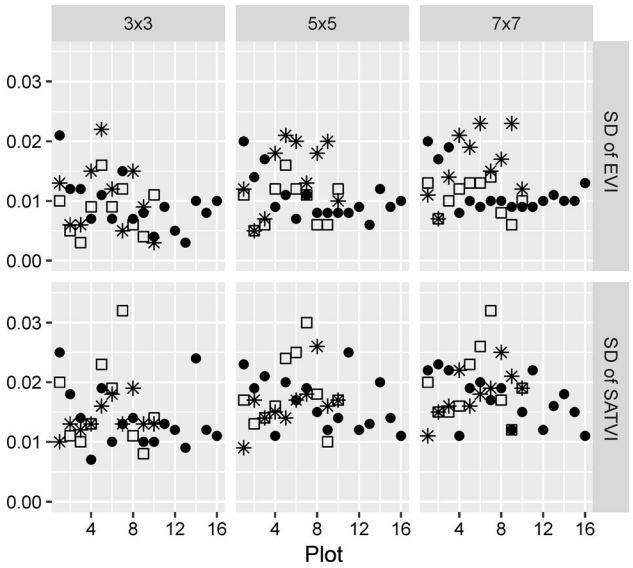
Conclusions

The response of passive and active remote sensors to the composition and structure of dry *R. girolae*-dominated woodlands, including shrub and tree biomass, abundance and variance in canopy cover of *R. girolae*, was investigated at sites with high climatic and topographic heterogeneity. Based on field-based data from 10 plots (50 × 30 m stand scale) at each study site (i.e. Ischigualasto Provincial Park, Valle Fértil Multiple Use Reserve and private land), for each plot we recorded richness (compositional indicator), abundance of shrubs and trees, abundance and variance in canopy cover of *R. girolae* (structural indicators). Passive remote sensing data included two green indices, Enhanced Vegetation Index (EVI) and Soil Adjusted Total Vegetation Index (SATVI), both obtained from L8 OLI, whereas active remote sensing data were backscatter coefficient values of VV co-polarisation and VH cross-polarisation, both obtained from Sentinel-1A. For each sampling field plot, we estimated standard deviation (SD) of passive and active remote sensing data within moving windows of different sizes (i.e. 3 × 3, 5 × 5 and 7 × 7), and this value was assigned to the central pixel of the moving window. In our study, richness was the only field-based data that had no relationship with remote sensing data, either passive or active, at any study site. Shrub biomass was explained by passive (57% in private land) and active (55% in Ischigualasto) remote sensing data. Increases in shrub biomass were related to a decrease in SD of EVI (at all scales) and an increase in SD of SATVI (7 × 7 moving window); moreover, they were related to a decrease in SD of VV and an increase in SD of VH polarisation (at all scales). In Valle Fértil, shrubs biomass was better explained by the multi-sensor model at the 3 × 3 moving window (46%) than by single-sensor models (26% passive and 27% active). Tree biomass was mainly explained by active remote sensing data. SD of VV polarisation and VH polarisation explained up to 83% of tree biomass variability in private land and up to 64% in Valle Fértil. Moreover, SD of VV and VH polarisation and SD of EVI and SATVI explained 90% of the variability in a multi-sensor model for private land. These results were probably due to variation in the signal produced by multiple bounces on trees of different species. *R. girolae* abundance was captured by passive remote sensors as homogeneous mature woodland, a negative relationship with SD of EVI and SATVI explained 31% of the variability in Ischigualasto. Moreover, SD of VV polarisation explained up to 37% of the variability in abundance of *R. girolae* in Ischigualasto, probably due to a different distribution of individuals. When significant variables of single-sensor models (i.e. SD of EVI, SATVI, and VV co-polarisation) were included in multi-sensor models, there was an increase in the explained variance (up to 54%), at the 3 × 3 moving window. The variability in *R. girolae* canopy was explained by higher variability in passive remote sensing data (i.e. SD of EVI and SATVI) in Ischigualasto (50%) and Valle Fértil (40%). The highest value for canopy variance was found in Ischigualasto (87% adults) and the lowest in Valle Fértil, where only 50% of individuals were adult trees, and the rest were seedlings and saplings. Further work is needed to assess the applicability of remote sensing data obtained from different passive and active sensors, using high-resolution spectral

or spatial satellite imagery. Additionally, biomass assessment could be improved by combining optical remote sensing and SAR imagery data. The multi-sensor models were better than single-sensor models to explain the attributes of these woodlands, except for the canopy variance of *R. girolae*. At any rate, as a first step, this work expands our understanding of the use of passive and active remotely sensed data as proxies for vegetation composition and structure in dry *R. girolae*-dominated woodlands.

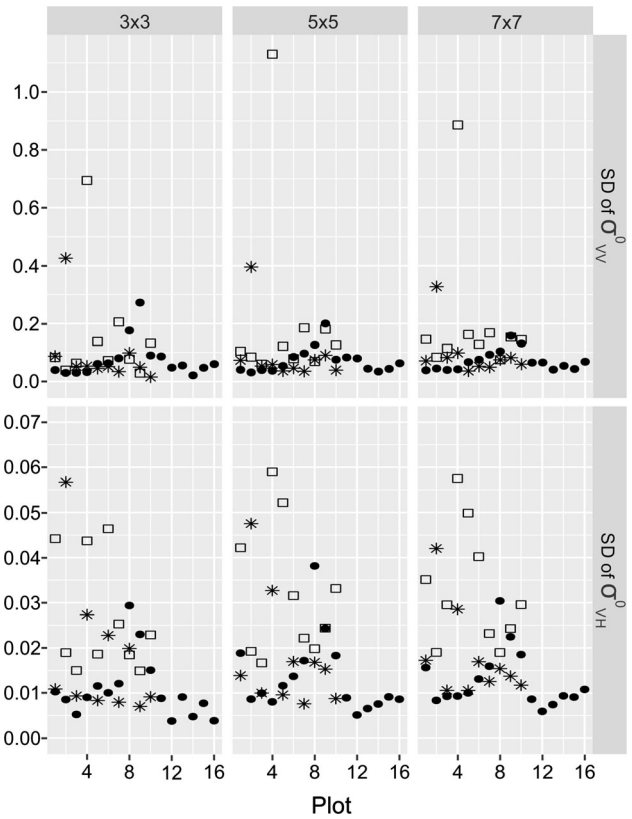
Appendix 1

Passive remote sensing data (*y*-axis) for each sampling field plot (*x*-axis). Passive remote sensing data are represented by Standard Deviation (SD) of EVI (Enhanced Vegetation Index) and SATVI (Soil Adjusted Total Vegetation Index). SD values were estimated considering 3×3, 5×5 and 7×7 moving windows (first, second and third column, respectively) for Ischigualasto (●), Valle Fértil (*) and private land (□).



Appendix 2

Active remote sensing data (*y*-axis) for each sampling field plot (*x*-axis). Active remote sensing data are represented by standard deviation (SD) of radar backscatter coefficient values (σ^0 expressed in original scale) in VH (cross-polarisation) and VV (co-polarisation). SD values were estimated considering 3×3, 5×5 and 7×7 moving windows (first, second and third column, respectively) for Ischigualasto (●), Valle Fértil (*) and private land (□).



Appendix 3

Multi-sensor models for Ischigualasto Provincial Park, Valle Fértil Multiple Use Reserve and private land, for field-based data (shrub and tree biomass, abundance of *R. girolae*) on *R. girolae*-dominated woodlands considering standard deviation (SD) of remote sensing data (i.e. SATVI, EVI, VV co-polarisation and VH cross-polarisation) as different predictor variables. Shown here are parameter estimates (± SE), *p*-values for significance (* = $p \leq 0.05$; ** = $p < 0.01$, *** = $p < 0.001$) and pseudo-R^2 for models.

Ischigualasto provincial park						
Field-based data	Moving window	Source image	Predictor/s	Estimate ± SE	*p*-value	pseudo-R^2
Abundance of *R. girolae*	3 × 3	L8 OLI	SATVI	− 0.27 ± 0.14	*	53.89
		Sentinel-1A	VV	0.22 ± 0.09	*	
Valle fértil multiple use reserve						
Shrubs biomass	3 × 3	L8 OLI	SATVI	− 0.16 ± 0.06	**	45.77
		Sentinel-1A	VH	− 0.18 ± 0.06	**	
Private land						
Shrubs biomass	3 × 3	L8 OLI	EVI	− 0.18 ± 0.07	**	58.84
		Sentinel-1A	VH	− 0.19 ± 0.07	**	
Trees biomass	7 × 7	L8 OLI	EVI	− 0.43 ± 0.16	**	89.59
		L8 OLI	SATVI	0.49 ± 0.15	**	
		Sentinel-1A	VV	− 2.07 ± 0.62	***	
		Sentinel-1A	VH	0.51 ± 0.13	***	

Acknowledgements We thank the staff of Ischigualasto Provincial Park and Valle Fértil Multiple Use Reserve for providing all the necessary facilities during fieldwork. We acknowledge and are grateful for the help received from members of INTERBIODES (Interacciones Biológicas del Desierto). Tomás Gonzalez assisted us in image processing. Nélida Horak assisted us in drafting the English version.

Funding This work was supported by National University of San Juan (Estado de los bosques de *Ramorinoa girolae* incluidos bajo distintas categorías de conservación en la provincia de San Juan), Res. N° 3635/15, and "Fondos para la Investigación Científica y Tecnológica, Plan Argentina Innovadora 2020" (Análisis de la dinámica espacio-temporal, composición y estructura de los bosques nativos de tierras secas en la provincia de San Juan), N° Resol-2018–310-APN-DANPCYT#MCT.

Declarations

Conflict of interest The authors have no competing interests to declare that are relevant to the content of this article. All authors certify that they have no affiliations with or involvement in any organisation or entity with any financial interest or non-financial interest in the subject matter or materials discussed in this manuscript.

References

Abatzoglou, J. T., Dobrowski, S. Z., Parks, S. A., & Hegewisch, K. C. (2018). TerraClimate, a high-resolution global dataset of monthly climate and climatic water balance from 1958–2015. *Scientific Data, 5*(1), 1–12. https://doi.org/10.1038/sdata.2017.191

Alvarez, J. A., Villagra, P. E., Cony, M. A., & Cesca, E. M. (2006). Estructura y estado de conservación de los bosques de Prosopis flexuosa D.C. (Fabaceae, Subfamilia: Mimosoideae) en el noreste de Mendoza (Argentina). *Revista Chilena De Historia Natural, 1*(79), 75–87. https://doi.org/10.4067/S0716-078X2006000100007

Bastin, J. F., Berrahmouni, N., Grainger, A., Maniatis, D., Mollicone, D., Moore, R., Patriarca, C., Picard, N., Sparrow, B. E., Abraham, M., Aloui, K., Atesoglu, A., Attore, F., Bassüllü, C., Bey, A., Garzuglia, M., García-Montero, L. G., Groot, N., Guerin, G., … Castro, R. (2017). The extent of forest in dryland biomes. *Science, 356*(6338), 635–638. https://doi.org/10.1126/science.aam6527

Bisigato, A. J., Villagra, P. E., Ares, J. O., & Rossi, B. E. (2009). Vegetation heterogeneity in monte desert ecosystems: A multi-scale approach linking patterns and processes. *Journal of Arid Environment, 73*(2), 182–191. https://doi.org/10.1016/j.jaridenv.2008.09.001

Bradley, B. A., Olsson, A. D., Wang, O., Dickson, B. G., Pelech, L., Sesnie, S. E., & Zachmann, L. J. (2012). Species detection vs. habitat suitability: Are we biasing habitat suitability models with remotely sensed data? *Ecological Modelling, 244*, 57–64. https://doi.org/10.1016/j.ecolmodel.2012.06.019

Brockerhoff, E. G., Jactel, H., Parrotta, J. A., & Ferraz, S. F. (2013). Role of eucalypt and other planted forests in biodiversity conservation and the provision of biodiversity-related ecosystem services. *Forest Ecology and Management, 301*, 43–50. https://doi.org/10.1016/j.foreco.2012.09.018

Brown, S. L., Schroeder, P., & Kern, J. S. (1999). Spatial distribution of biomass in forests of the Eastern USA. *Forest Ecology and Management, 123*(1), 81–90. https://doi.org/10.1016/S0378-1127(99)00017-1

Brown, A., Martinez, Ortiz, U., Acerbi, M., Corcuera, J., & Pacheco, S. (2006). *La Situación Ambiental Argentina 2005*. Fundación Vida Silvestre Argentina, Buenos Aires.

Campos, V. E., Gatica, G., & Bellis, L. M. (2015). Remote sensing variables as predictors of habitat suitability of the Viscacha Rat (*Octomys Mimax*), a rock-dwelling mammal living in a desert environment. *Mammal Research, 60*(2), 117–126. https://doi.org/10.1007/s13364-015-0215-3

Campos, V. E., Cappa, F. M., Fernández Maldonado, V., & Giannoni, S. M. (2016). Using remotely sensed data to model suitable habitats for tree species in a desert environment. *Journal of Vegetation Science, 27*(1), 200–210. https://doi.org/10.1111/jvs.12328

Campos, V. E., Fernández Maldonado, V., Balmaceda, P., & Giannoni, S. (2017). Richness of plants, birds and mammals under the canopy of *Ramorinoa Girolae*, an endemic and

vulnerable desert tree species. *Bosque, 38*(2), 307–316. https://doi.org/10.4067/S0717-92002017000200008

Campos, V. E., Gatica, G. M., Cappa, F. M., Giannoni, S. M., & Campos, C. M. (2018). Remote sensing data to assess compositional and structural indicators in dry woodland. *Ecological Indicators, 88*, 63–70. https://doi.org/10.1016/j.ecolind.2018.01.032

Campos, V. E., Cappa, F. M., Gatica, G. M., & Campos, C. M. (2020). Drivers of plant species richness and structure in dry woodland of *Prosopis flexuosa*. *Acta Oecologica*. https://doi.org/10.1016/j.actao.2020.103654

Cesca, E., Villagra, P. E., Passera, C. B., & Alvarez, J. A. (2012). Effect of *Prosopis Flexuosa* on understory species and its importance to pastoral management in woodlands of the central monte desert. *Revista De La Facultad De Ciencias Agrarias, 44*(2), 207–219.

Crabbe, R. A., Lamb, D. W., Edwards, C., Andersson, K., & Schneider, D. (2019). A preliminary investigation of the potential of sentinel-1 radar to estimate pasture biomass in a Grazed, Native Pasture Landscape. *Remote Sensing, 11*(7), 872. https://doi.org/10.3390/rs11070872

Crawley, M. J. (2007). *The R Book*. Wiley.

Flores-Anderson, A.I., Herndon, K. E., Thapa, R. B., & Cherrington, E. (2019). SAR Handbook: Comprehensive Methodologies for Forest Monitoring and Biomass Estimation. *NASA*.

Gaitán, J. J., Bran, D., Oliva, G., Ciari, G., Nakamatsuc, V., Salomone, J., Ferrante, D., Buono, G., Massarad, V., Humano, G., Celdrán, D., Opazoc, W., & Maestre, F. T. (2013). Evaluating the performance of multiple remote sensing indices to predict the spatial variability of ecosystem structure and functioning in Patagonian steppes. *Ecological Indicators, 34*, 181–191. https://doi.org/10.1016/j.ecolind.2013.05.007

Gao, X., Huete, A. R., Ni, W., & Miura, T. (2000). Optical–biophysical relationships of vegetation spectra without background contamination. *Remote Sensing of Environment, 74*, 609–620. https://doi.org/10.1016/S0034-4257(00)00150-4

Goirán, S. B., Aranibar, J. N., & Gomez, M. L. (2012). Heterogeneous spatial distribution of traditional livestock settlements and their effects on vegetation cover in arid groundwater coupled ecosystems in the Monte Desert (Argentina). *Journal of Arid Environment, 87*, 188–197. https://doi.org/10.1016/j.jaridenv.2012.07.011

Hadad, M., Almiron, M., & Scaglia, J. (2014). Estructura de Un Bosque de *Ramorinoa girolae* (Fabaceae), En La Sierra de Pie de Palo, San Juan (Argentina). *Boletín De La Sociedad Argentina De Botánica, 49*(2), 283–292. https://doi.org/10.31055/1851.2372.v49.n2.7860

Hall, R. J., Skakun, R. S., Arsenault, E. J., & Case, B. S. (2006). Modeling forest stand structure attributes using landsat ETM+ data: Application to mapping of aboveground biomass and stand volume. *Forest Ecology and Management, 225*(1–3), 378–390. https://doi.org/10.1016/j.foreco.2006.01.014

Hansen, M. C., Potapov, P. V., Moore, R., Hancher, M., Turubanova, S. A., Tyukavina, A., Thau, D., Stehman, S. V., Goetz, S. J., Loveland, T. R., Kommareddy, A., Egorov, A., Chini, L., Justice, C. O., & Townshend, J. R. G. (2013). High-resolution global maps of 21st-century forest cover change. *Science, 342*(6160), 850–853. https://doi.org/10.1126/science.1244693

Huete, A., Didan, K., Miura, T., Rodriguez, E. P., Gao, X., & Ferreira, L. G. (2002). Overview of the radiometric and biophysical performance of the MODIS vegetation indices. *Remote Sensing of Environment, 83*(1), 195–213. https://doi.org/10.1016/S0034-4257(02)00096-2

Huete, A. (1988). A soil-adjusted vegetation index (SAVI). *Remote Sensing of Environment, 22*(1), 295–309. https://doi.org/10.1016/0034-4257(88)90106-X

Irisarri, J. G. N., Oesterheld, M., Paruelo, J. M., & Texeira, M. (2012). Patterns and controls of aboveground net primary production in meadows of Patagonia. A remote sensing approach. *Journal of Vegetation Science, 23*(1), 114–126.

Kiesling, R. (1994). *Flora de San Juan. Pteridófitas, Gimnospermas. Dicotiledóneas Dialipétalas (Salicáceas-Leguminosas).* Volumen I. Vazquez Mazzini Editorial, Buenos Aires.

Latifi, H., Fassnacht, F. E., Hartig, F., Berger, C., Hernández, J., Corvalán, P., & Koch, B. (2015). Stratified aboveground forest biomass estimation by remote sensing data. *International Journal of Applied Earth Observation and Geoinformation, 38*, 229–241. https://doi.org/10.1016/j.jag.2015.01.016

Laurin, G. V., Balling, J., Corona, P., Mattioli, W., Papale, D., Puletti, N., Rizzo, M., Truckenbrodt, J., & Urban, M. (2018). Aboveground biomass prediction by sentinel-1 Multitemporal Data in Central Italy with Integration of ALOS2 and Sentinel. *Journal of Applied Remote Sensing*. https://doi.org/10.1117/1.JRS.12.016008

Lawley, V., Lewis, M., Clarke, K., & Ostendorf, B. (2015). Site-based and remote sensing methods for monitoring indicators of vegetation condition: An australian review. *Ecological Indicators, 60*, 1273–1283. https://doi.org/10.1016/j.ecolind.2015.03.021

Lu, D., Chen, Q., Wang, G., Liu, L., Li, G., & Moran, E. (2014). A survey of remote sensing-based aboveground biomass estimation methods in forest ecosystems. *International Journal of Digital Earth, 9*(1), 63–105. https://doi.org/10.1080/17538947.2014.990526

Marsett, R. C., Qi, J., Heilman, P., Biedenbender, S. H., Carolyn, M., Amer, S., Weltz, M., Goodrich, D., Marsett, R., & Watson, M. C. (2006). Remote sensing for grassland in the arid management Southwest. *Rangeland Ecology and Management, 59*(5), 530–540. https://doi.org/10.2111/05-201r.1

Mendes, F. S., Baron, D., Gerold, G., Liesenberg, V., & Erasmi, S. (2019). Optical and SAR remote sensing synergism for mapping vegetation types in the Endangered Cerrado/Amazon Ecotone of Nova Mutum—Mato Grosso. *Remote Sensing, 11*, 1161–1186. https://doi.org/10.3390/rs11101161

Millennium Ecosystem Assessment. (2005). *Ecosystems and human well-being: Synthesis*. Island Press.

Nagendra, H. (2001). Using remote sensing to assess biodiversity. *International Journal of Remote Sensing, 22*(12), 2377–2400. https://doi.org/10.1080/01431160117096

Noss, R. F. (1990). Indicators for monitoring biodiversity–a hierarchical approach. *Conservation Biology, 4*, 355–364. https://doi.org/10.1111/j.1523-1739.1990.tb00309.x

Papú, S. S., Lagos, S., & Campos, C. M. (2015). Pre-dispersal seed loss of *Ramorinoa girolae* (Fabaceae) in Ischigualasto Provincial Park (San Juan, Argentina). *Boletín De La Sociedad Argentina De Botánica, 50*(4), 585–594. https://doi.org/10.31055/1851.2372.v50.n4.12917

Pasiecznik, N.M., Felker, P., Harris, P.J.C., Harsh, L.N., Cruz, G., Tewari, J.C., Cadorte, K., & Maldonado, L.J. (2001). *The Prosopis juliflora - Prosopis pallida complex: a Monograph.* Henry Doubleday Research Association, Coventry, United Kingdom.

Passera, C., Dalmasso, A. D., & Borsetto O. (1983). Método del Point Quadrat Modificado, in: *Taller sobre arbustos forrajeros (FAO-IADIZA).* Mendoza, Argentina, pp. 135–151.

Pyke, D. A., Pellant, M., Shaver, P., & Herrick, J. E. (2002). Rangeland health attributes and indicators for qualitative assessment. *Journal of Range Management, 55*, 584–597. https://doi.org/10.2307/4004002

Piraino, S., Abraham, E. M., Diblasi, A., & Roig Juñent, F. A. (2015). Geomorphological-related heterogeneity as reflected in tree

growth and its relationships with climate of monte desert *Prosopis Flexuosa* DC Woodlands. *Trees, 29*(3), 903–916.

Quantum GIS Version 3.4.8 "Madeira" Development Team, 2018. QGIS Geographic Information System. Open Source Geospatial Foundation Project. http://qgis.osgeo.org/

R Core Team, 2019. A language and environment for statistical computing. R Foundation for Statistical Computing. Vienna, Austria. URL. http://www.R-project.org/

Ribeiro, P. J. Jr., Diggle, P. J., Schlather, M., Bivand, R., & Ripley, B. (2016). geoR: Analysis of Geostatistical Data. R package version 1.8–1. https://CRAN.R-project.org/package=geoR

Rocchini, D., Chiarucci, A., & Loiselle, S. A. (2004). Testing the spectral variation hypothesis by using satellite multispectral images. *Acta Oecologica, 26*(2), 117–120. https://doi.org/10.1016/j.actao.2004.03.008

Rossi, B., & Villagra, V. E. (2003). Effects of *Prosopis flexuosa* on soil properties and the spatial pattern of understorey species in Arid Argentina. *Journal of Vegetation Science, 14*(4), 543–550. https://doi.org/10.1658/1100-9233(2003)014[0543:eopfos]2.0.co;2

Schloerke, B., Crowley J., Cook D., Briatte F., Marbach M., Thoen E., Elberg A., & J. Larmarange. (2020). "Package GGally". https://CRAN.R-project.org/package=GGally

Smith, W. K., Dannenberg, M. P., Yang, D., Herrmann, S., Barnes, M. L., Barron-Gafford, G. A., Biederman, J. A., Ferreberg, S., Fox, A. M., Hudson, A., Knowles, J. F., MacBean, N., Moore, D. J. P., Nagler, P. L., Reed, S. C., Rhuterford, W. A., Scott, R. L., Wang, X., & Yang, J. (2019). Remote sensing of dryland ecosystem structure and function: Progress, challenges, and opportunities. *Remote Sensing of Environment, 233*, 111401. https://doi.org/10.1016/j.rse.2019.111401

Thompson, I. D., Okabe, K., Tylianakis, J. M., Kumar, P., Brockerhoff, E. G., Schellhorn, N. A., Parrotta, J. A., & Nasi, R. (2011). Forest biodiversity and the delivery of ecosystem goods and services: Translating science into policy. *BioScience, 61*(12), 972–981. https://doi.org/10.1525/bio.2011.61.12.7

Venables, W. N., & Ripley, B. D. (2002). Modern applied statistics with S-Plus. *The American Statistician, 53*(1), 86–87. https://doi.org/10.2307/2685660

Villagra, P. E. (2000). Aspectos Ecológicos De Los Algarrobales Argentinos. *Multequina, 9*(2), 35–51.

Zapata, R. M. (2017). Distribución y Caracterización de Poblaciones Naturales de 'Chica' (*Ramorinoa Girolae* Speg., Fabaceae), Especie Endémica de Argentina, y Valoración Alimenticia de Sus Semillas. *PhD diss., Universidad Nacional de Córdoba.*

Zar, J. (1999). *Biostatistical Analysis*. Pearson Prentice Hall, E.E.U.U.

Zenner, E. K., & Hibbs, D. E. (2000). A new method for modeling the heterogeneity of forest structure. *Forest Ecology and Management, 129*, 75–87. https://doi.org/10.1016/S0378-1127(99)00140-1

Zhao, P., Lu, D., Wang, G., Liu, L., Li, D., Zhu, J., & Yu, S. (2016). Forest aboveground biomass estimation in zhejiang province using the integration of landsat TM and ALOS PALSAR Data. *International Journal of Applied Earth Observation and Geoinformation, 53*, 1–15. https://doi.org/10.1016/j.jag.2016.08.007

Zhu, Z., Woodcock, C. E., & Olofsson, P. (2012). Continuous monitoring of forest disturbance using all available landsat imagery. *Remote Sensing of Environment, 122*, 75–91. https://doi.org/10.1016/j.rse.2011.10.030

Zuur, A. F., Ieno, E. N., Walker, N. J., Saveliev, A. A., & Smith, G. M. (2009). *Mixed effects models and extensions in ecology with R*. Springer Science. https://doi.org/10.1007/978-0-387-87458-6

Publisher's Note Springer Nature remains neutral with regard to jurisdictional claims in published maps and institutional affiliations.